Int J Clin Exp Pathol 2017;10(2):1019-1029
www.ijcep.com /ISSN:1936-2625/IJCEP0040296

Original Article

An RNA-Seq screen of the dithiothreitol-induced apoptosis response in chicken cardiomyocytes

Chunyun Wan[1,2*], Jinmei Xiang[2,3*], Rui Guo[4], Shijin Yang[2], Youwen Li[2], Dingzong Guo[2]

[1]College of Animal Science, Yangtze University, Jingzhou, Hubei, China; [2]College of Veterinary Medicine, Huazhong Agricultural University, Wuhan, Hubei, China; [3]Department of Animal Science, Hubei Vocational College of Bio-Technology, Wuhan, Hubei, China; [4]Hubei Key Laboratory of Embryo and Molecular Breeding, Hubei Academy of Agricultural Sciences, Wuhan, Hubei, China. [*]Equal contributors.

Received September 20, 2016; Accepted September 27, 2016; Epub February 1, 2017; Published February 15, 2017

Abstract: Cardiomyocytes in postnatal heart are terminally differentiated and thus possess limited capacity to regenerate. Loss of cardiomyocytes through apoptosis and necrosis can lead to heart failure and other serious consequences. Compared to mammals, substantially less research has been conducted on chicken cardiomyocytes; thus, the apoptosis pathways and many relevant genes remain unknown. To elucidate the pathways and genes involved in chicken myocardial cell apoptosis, primary cultures of chicken embryo cardiomyocytes were sham-treated or exposed to the apoptosis inducer dithiothreitol (DTT), and RNA-Seq with technical replicates conducted to identify differentially expressed genes and transcripts. Relevant differentially expressed transcripts were used to construct a protein-protein interactive network for chicken apoptosis. Sequencing detected a total of 19,268 known genes and 2,160 novel genes. In the DTT treatment group, 6468 genes showed significant differential expression based on DEseq analysis, of which 47.99% were upregulated and 52.01% downregulated. The initiation of apoptosis was primarily dependent on *caspase-8* and *caspase-9*, whereas the execution stage was dependent on *caspase-3*. Upregulated genes also included many involved in the *WNT* and *MAPK* pathways. Repression of apoptosis was primarily dependent on *Bcl-2*, *IAP*, and *SIVA*. These results provide a foundation for detailed analysis of avian myocardial apoptosis, including genes and LncRNAs that constitute, regulate, or link various pro- and anti-apoptotic pathways.

Keywords: RNA-Seq, apoptosis, cardiomyocytes, apoptosis inducer, DTT

Introduction

Myocardial cell apoptosis is a critical pathogenic process in many types of heart disease. Apoptotic cardiomyocytes lose their contractility and gradually exhibit reduced function, leading to heart failure [1-3]. Tan and colleagues reported that broilers with higher rates of growth exhibit abnormally elevated myocardial cell apoptosis, leading heart failure and ascites syndrome [4]. Therefore, myocardial cell apoptosis may limit commercial productivity.

To date, most studies on myocardial cell apoptosis have been performed in mammals. As a result, mammalian apoptosis pathways are well established, such as the death receptor pathway [5] and the mitochondrial signaling pathway [6, 7]. Many general apoptosis-associated genes and molecules have been identified, such as members of the caspase family [8], as well as cardiomyocyte-specific molecules like apoptosis repressor with CARD domain (ARC) [9]. However, there has been little relevant research on chickens, so apoptosis pathways remain unclear. Moreover, certain key apoptosis genes observed in mammals have not been found in chicken heart.

The sequencing of mRNA transcripts (termed RNA-Seq) is a well-developed technology that has been widely used in recent years to screen for differentially expressed genes, including those without prior annotation [10-12]. However, few RNA-seq studies have been conducted in chickens. Although some work has been conducted on chicken resistance to *Campylobacter jejuni* colonization using mRNA sequencing [13], this phenomenon is unrelated to apoptosis in cardiomyocytes.

In the late-stage chicken embryo, heart development is nearly complete, and the number of cardiomyocytes rarely increases thereafter, so primary cells isolated at this stage are thought to express similar apoptotic signaling pathways as mature cardiomyocytes in vivo [14-16].

Dithiothreitol (DTT) is a reducing agent that can induce apoptosis by activating caspase-3 [17]. To identify the apoptotic pathways present in chicken cardiomyocytes and any novel genes involved, apoptosis was induced using DTT and RNA samples were sequenced using 100-bp paired-end reads on the Illumina Hiseq 2000 platform. Functions of differentially expressed genes were analyzed by GO and KEEG, and protein-protein networks constructed using STRING.

Materials and methods

Pretreatment and apoptosis induction in primary cardiomyocytes from chicken embryos

Monolayer cultures of embryonic chicken cardiomyocytes were prepared by the methods of DeHaan with some modifications [18-20]. Briefly, White Leghorn eggs were obtained from Beijing Merial Vital Laboratory Animal Technology (Beijing, China). At embryonic day 14 (E14), embryos were removed and decapitated in a Petri dish filled with Medium 199/EBSS (HyClone, Logan, Utah, USA) supplemented with 3% fetal bovine serum (FBS, Gibco, Grand Island, New York, USA). Ventricular tissues were isolated, pooled, and treated with 0.05% trypsin-EDTA to obtain a cell suspension as described [21]. We used the differential attachment technique to obtain high purity cells after 0.5 h of incubation. Cells were incubated in growth medium (Medium 199/EBSS containing 10% FBS) at 37°C under a 5% CO_2 atmosphere. Cultures were washed three times at 8, 24, and 48 h to remove dead and dying cells. The serum concentration in the medium was then changed from growth (10%) to maintenance (2%) conditions, and incubation was continued for 36 h. The cells were then divided into two groups: a control group and an experimental group treated with 2 mM DTT for 10 h. The DTT dose and exposure time were determined by prior testing and by referencing previous studies [17]. The degree of apoptosis was estimated by DAPI staining. The control group was treated in the same way but with omission of DTT. All individual treatments were repeated twice; replicates were named_1 and _2, respectively (e.g., DTT_1 and DTT_2). The RNA sample obtained from each replicate was bi-directionally sequenced, for four sequencing results per sample (named accordingly as DTT_1_1, DTT_1_2, DTT_2_1, and DTT_2_2).

RNA sample collection and preparation

Total RNA was extracted using standard protocols (TRIzol, Invitrogen, CA, USA) and treated with DNase to remove any potential genomic DNA contamination. The quality of RNA was monitored by electrophoresis on 1% agarose gels. RNA purity and concentration were checked using a NanoPhotometer spectrophotometer (Implen, CA, USA) and Qubit RNA Assay Kit in a Qubit 2.0 Fluorometer (Life Technologies, CA, USA). RNA integrity was assessed using the Bioanalyzer 2100 system (Agilent Technologies, CA, USA).

Library preparation for transcriptome sequencing

After total RNA extraction, mRNA was purified using poly-T oligo-attached magnetic beads [13]. Briefly, 3 μg of RNA was used as the input for each RNA sample preparation. Sequencing libraries were generated using a NEB Next Ultra RNA LibraryPrep Kit (Illumina, NEB, USA) following the manufacturer's instructions. Index codes were assigned to attribute the sequences to each sample.

Clustering of the index-coded samples was performed on a cBot Cluster Generation System (Illumina) according to the manufacturer's instructions. After cluster generation, the library preparations were sequenced on anIllumina HiSeq 2000 platform, and 100-bp paired-end reads were generated [22].

Sequencing quality control and reads mapping to the reference genome

After sequencing, raw data in fastq format were first processed through in-house perl scripts. In this step, clean data were obtained by removing low-quality reads and reads containing the adapter sequence or poly-N. At the same time, Q20, Q30, and the GC content of the clean data were calculated. All subsequent analyses were based on these clean datasets.

Reference genome and gene model annotation files were directly downloaded from the Genome

Table 1. Major characteristics of RNA-seq in the Dithiothreitol (DTT) and Control group

Sample name	Raw reads	Clean reads	Clean bases	Error rate (%)	Q20 (%)▲	Q30 (%)▲	GC content (%)*
Control_1_1	61286178	57687170	5.77G	0.03	97.15	91.50	53.26
Control_1_2	61286178	57687170	5.77G	0.04	96.03	89.60	53.32
Control_2_1	57289438	53642113	5.36G	0.04	97.03	91.19	54.04
Control_2_2	57289438	53642113	5.36G	0.04	95.75	88.93	54.09
DTT_1_1	60625569	56773931	5.68G	0.04	97.06	91.21	54.16
DTT_1_2	60625669	56773931	5.68G	0.04	95.88	89.13	54.23
DTT_2_1	58512360	55415481	5.54G	0.03	97.45	92.14	52.55
DTT_2_2	58512360	59247377	5.54G	0.04	96.43	90.38	52.60

▲Q20 (%) and Q30 (%) are the percentages of reads with Phred quality scores > 20 and > 30, respectively. *GC content (%) is G+C bases as a percentage of total bases.

Table 2. Alignment between reads and reference genome

Sample name	Control_1	Control_2	DTT_1	DTT_2
Total reads	115374340	107284226	113547862	110830962
Total mapped	91503521 (79.31%)	83841695 (78.15%)	88185209 (76.66%)	89930237 (81.14%)
Multiple mapped	1600343 (1.39%)	1402762 (1.31%)	1290942 (1.14%)	1249805 (1.13%)
Uniquely mapped	89903178 (77.92%)	82438933 (76.84%)	86894267 (76.53%)	88680432 (80.01%)
Read-1	45188675 (39.17%)	41417088 (38.61%)	43660592(38.45%)	44552779 (40.20%)
Read-2	44714503 (38.76%)	41021845 (38.24%)	43233675 (38.08%)	44127653 (39.82%)
Reads map to '+'	44938933 (38.95%)	41207084 (38.41%)	43406284 (38.23%)	44320942 (39.99%)
Reads map to '-'	44964245 (38.97%)	41231849 (38.43%)	43487983 (38.3%)	44359490 (40.02%)
Non-splice reads	55928960 (48.48%)	50563133 (47.13%)	52566632 (46.29%)	53055356 (47.87%)
Splice reads	33974218 (29.45%)	31875800 (29.71%)	34327635 (30.23%)	35625076 (32.14%)

Reads map to '+', Reads map to '-': reads to positive and negative chain of Genome, read-1, -2: repeat sequencing of each sample.

website (http://www.ncbi.nlm.nih.gov/genome/111?project_id=10808). An index of the reference genome was built using Bowtie v2.0.6, and paired-end clean reads were aligned to the reference genome using TopHat v2.0.9 [22].

Quantification of gene expression levels

The reads mapped to each gene were counted by HTSeq v0.5.4p3. The RPKM (reads per kilobase of the exon model per million mapped reads) of each gene was then calculated based on gene length and read counts mapped. This method considers the effects of sequencing depth and gene length for the read counts and is currently the most reliable method for estimating gene expression levels [21].

Alternative splicing and differential expression analysis

Alternative splicing was determined by Cufflinks 2.1.1 and ASprofile 1.0 software. Differential expression analysis was performed using the DESeqR package (1.10.1). DESeq provides statistical methods for determining differential expression in digital gene expression data using a model based on the negative binomial distribution. The resulting *P*-values were adjusted using Benjamini and Hochberg's approach for controlling the false discovery rate; that is, genes with an adjusted P<0.05 by DESeq were classified as differentially expressed. Corrected *P* values of 0.005 and log2 (fold change) values of 1 were set as the threshold for significant differential expression.

GO and KEGG enrichment analysis of differentially expressed genes

After functional annotation, genes were further classified by Gene Ontology (GO) assignments. GO enrichment analysis of differentially expressed genes was performed using the GOseq R package, in which gene length bias was corrected. GO terms with corrected P<0.05 were considered significantly enriched in differentially expressed genes [23].

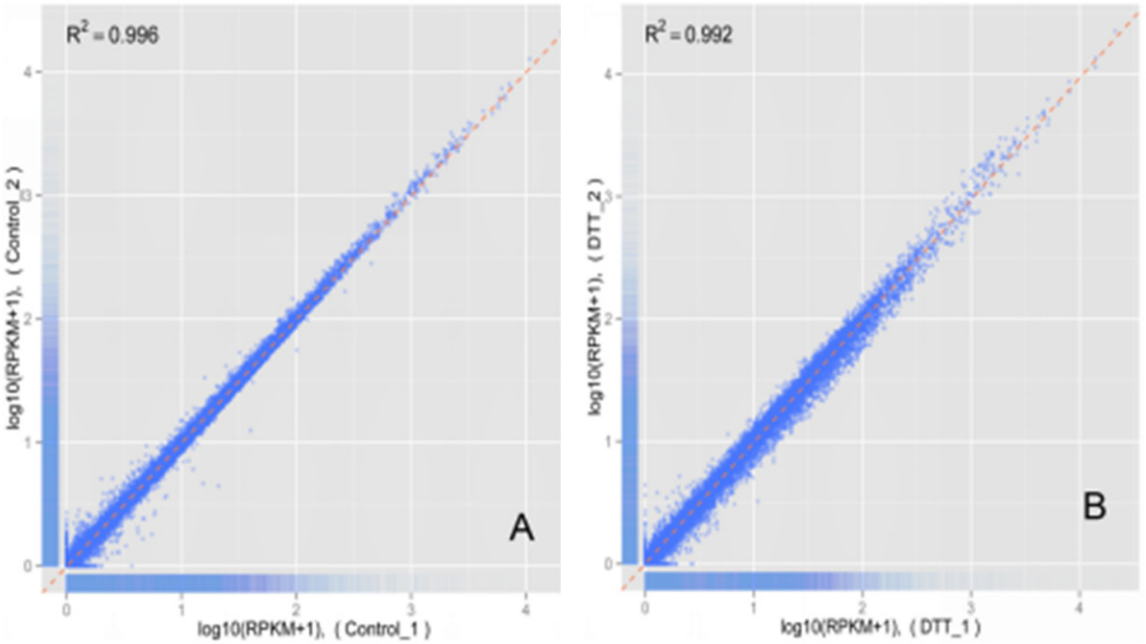

Figure 1. Correlations among technical replicates in each group. R^2: square of the Pearson correlation coefficient.

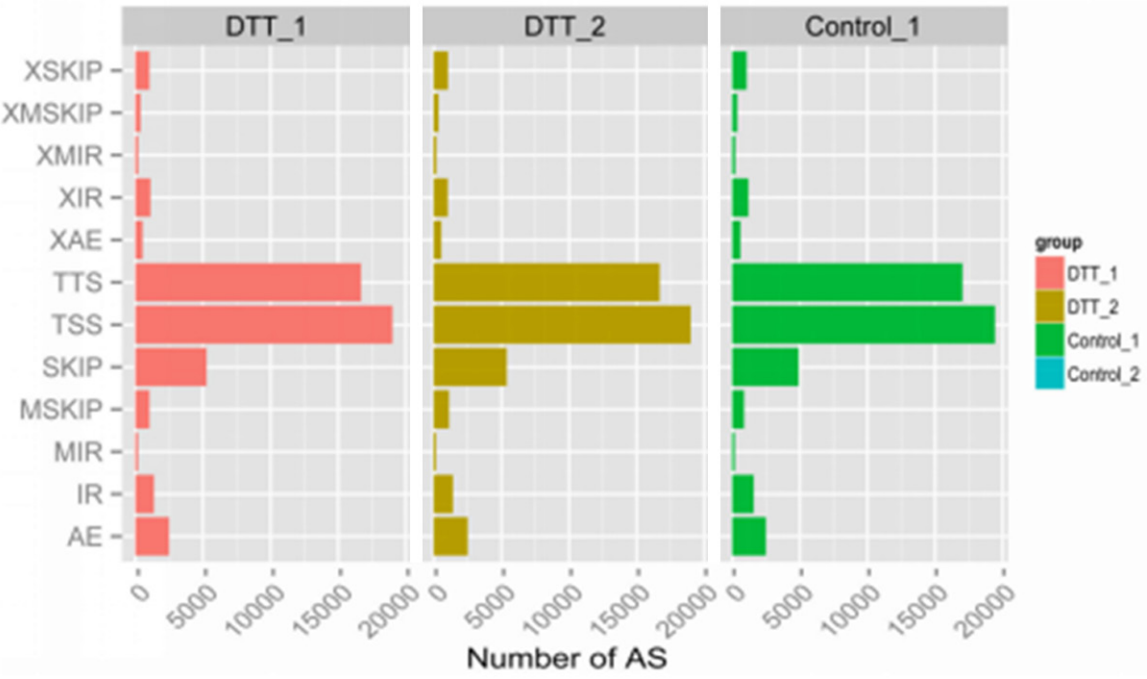

Figure 2. Statistics of the different alternative splicing events. The abbreviations indicate the different types of alternative splicing events as follows: SKIP: skipped exon; XSKIP: approximate SKIP; MSKIP: multi-exon SKIP; XMSKIP: approximate MSKIP; IR: intron retention; MIR: multi-IR; XMIR: approximate MIR; XIR: approximate IR; AE: alternative exon ends; XAE: approximate AE; TSS: alternative 5' first exon; TTS: alternative 3' last exon.

The Kyoto Encyclopedia of Genes and Genomes (KEGG) is a database resource for the hierarchal categorization of genes and gene groups identified from genome sequencing and other high-throughput methods (http://www.genome.jp/kegg/). We used KOBAS software to test the

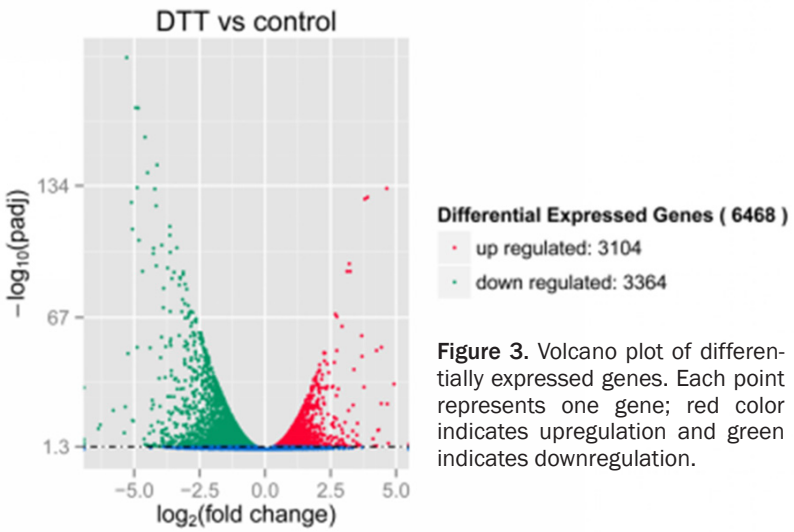

Figure 3. Volcano plot of differentially expressed genes. Each point represents one gene; red color indicates upregulation and green indicates downregulation.

Table 3. Primers used for the qPCR analysis

Gene	Forward	Reverse
AMPN	TGCAGCACTGAGACCTGGAT	CAGTTGCTGCGGATGAAGTC
EGLN	CGAGGCCATCAACTTCCTTC	TCCACATGACGCACATACCC
DDX4	TCTTGTGGCAACTTCGGTAGC	ACGACCAGTTCGTCCAATTCG
FGF10	AGACACGTGCGGAGCTACAAT	ACCTTGCCGTTCTTCTCGAT
FOXO3	ACAAACCGTGCACTGTGGAGT	TGGAGCTTCTCTGCATCATCC
GHOX7	TTGATCAGAACATTCCCGTCC	GGAAATTAGCCTCAGCCTGGT
TGFBR	AGACTGCAGCGATGTTTGTGC	GGCAGCAATTCTGTGTTGTGG
NF-κB	GGACTTAAAATGGCAGGAGAG	GCTGTTCGTAGTGGTAAGTCTG
MAPK	GCGGCTCCGCTAAAATGCCG	GGGGTGAGGTTCTGGTAGCGC
CASP8	ACTGACATGGACTGAAGGA	TTACAGTGACGTGCTCCA
CASP9	TCAGACATCGTATCCTCCA	AAGTCACAGCAGGGACA
CASP3	GATGCTGCAAGTGTCAGA	ATCGCCATGGCTTAGCA
Bcl	GCTTTGAGCAGGTAGTGA	CAAGTACGTGGTCATCCAA
Bcl-2	TGAGCAGAGGTCACGTA	CACACTGTGGAACAGCA
CytC	CCTGTCCTGGTGCATGATG	TACTCTGATCCAGCTCTGCCTGAA
BAK1	GCCCTGCTGGGTTTCGGTAA	AATTCGGTGACGTAGCGGGC
TNFRSF	CCTGCTCCTCATCATTGTGT	TGATCCATGTACTCCTCTCC
P53	ACCTGCACTTACTCCCCGGT	TCTTATAGACGGCCACGGCG
XIAP	GGGCATCACATAGGAGCGCA	TCCTTCCACTCTTGCAATCC
β-actin	CTGATGGTCAGGTCATCACCATT	ACCCAAGAAAGATGGCTGGA

statistical enrichment of differentially expressed genes in KEGG pathways [24, 25].

Novel transcript prediction and alternative splicing analysis

The Cufflinks v2.1.1 Reference Annotation Based Transcript (RABT) assembly method was used to construct and identify both known and novel transcripts from the TopHat alignment results. Alternative splicing events were classified into 12 basic types by ASprofile v1.0. The number of AS events was estimated separately in each sample.

SNP analysis

We used Picard-tools v1.96 and SAM tools v0.1.18 to sort and identify duplicated reads and reorder the BAM alignment results for each sample. The GATK2 software was used for SNP calling.

Results

Sequencing quality control

After RNA sequencing, we assessed the quality of the data. The Q20, Q30, and GC content in the clean data were calculated (**Table 1**). Alignments between reads and the reference genome are presented in **Table 2**. Replicates of each sample were sequenced, and the correlations between replicates are shown in **Figure 1**.

Alternative splicing and differential expression analysis

Alternative splicing (AS) analysis was performed using Cufflinks 2.1.1 and ASprofile 1.0. The alternative splicing event statistics are shown in **Figure 2**. The most common AS types were TSS (alternative 5' first exon) and TTS (alternative 3' last exon). We found some genes with more than five AS types.

To assess global transcriptional changes associated with apoptosis induction, we applied previously described methods [21] to identify differentially expressed genes from the normalized

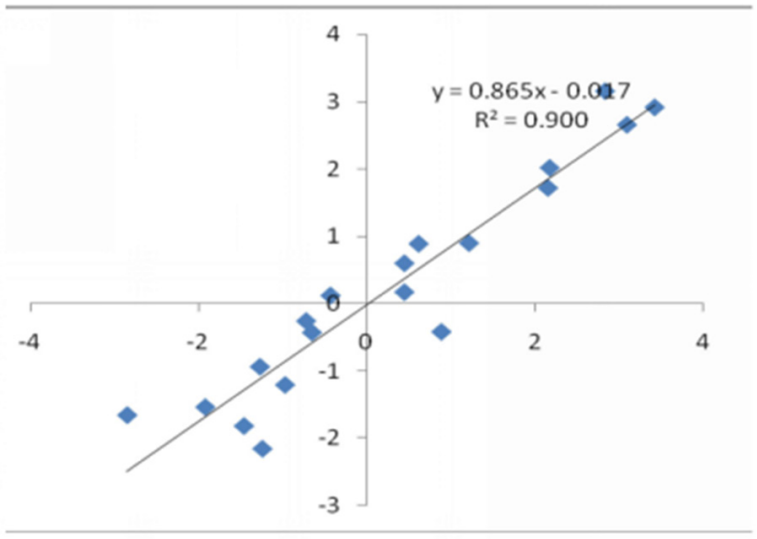

Figure 4. Validation of the RNA-Seq approach using qPCR. Nineteen genes that were differentially expressed between the DTT and control groups (10 upregulated and 9 downregulated) were selected. Their levels of expression were quantified by qRT-PCR analysis. The log2 changes in expression for the qRT-PCR and RNA-Seq data were closely correlated (r^2=0.900; P<0.01), confirming the accuracy of the RNA-Seq approach for quantification.

data. The results showed that 6468 genes were significantly differentially expressed between control and DTT-treated cultures. A volcano plot of differential gene expression (**Figure 3**) shows that 47.99% of all differentially expressed genes were upregulated and 52.01% downregulated.

Validation of differential gene expression data by qPCR

To validate the differentially expressed genes identified by sequencing, we selected 19 genes for qPCR confirmation, including 9 downregulated genes (*AMPK, EGLN1, DDX4, FGF10, FOXO3, GHOX4.7, TGFBR, NF-κB, and MAPK*) and 10 upregulated genes (*CASP8, CASP9, CASP3, Bcl, Bcl2, BAK1, TNFRSF1A, CytC, P53, and XIAP*). The primers for the qPCR assays are shown in **Table 3**. For the selected gene population, there was a strong correlation between RNA-Seq and qPCR results (r^2=0.900) (**Figure 4**), confirming the reliability of differential expression analysis using RNA-Seq.

GO and KEGG enrichment analyses of differentially expressed genes

GO enrichment analysis of differentially expressed genes was performed using the GOseq R package. GO terms with corrected P<0.05 were considered significantly enriched in differentially expressed genes. Genes were categorized into 11510 GO terms within three domains: 'biological process', 'cellular component', and 'molecular function' (**Figure 5**). In the 'biological process' domain, the GO terms with highest enrichment of differentially expressed genes were 'regulation of response to stimulus', 'response to stress', and 'macromolecule localization'. In the cell 'component domain', terms with highest enrichment were 'intracellular', 'cell', and 'cell part'. We also observed a high percentage of differentially expressed genes assigned to 'intracellular signal transduction', 'regulation of signal transduction', and 'regulation of cell communication'. Alternatively, few genes were assigned to categories thought unrelated to apoptosis, such as 'cyanoamino acid metabolism'.

We also analyzed the biological pathways that were modulated during apoptosis in our samples. The genes were assigned to 152 pathways in the KEGG database. A few pathways, including the cytokine-cytokine receptor interaction pathway, *MAPK* signaling pathway, metabolic pathways, and regulation of the actin cytoskeleton pathway, contained large numbers of differentially expressed genes, while others, such as sulfur metabolism, contained only a few (**Figure 6**).

Discussion

Cardiomyocytes are terminally differentiated during the late embryonic period; thus, the myocardium has limited regenerative capacity throughout postnatal life. Apoptosis and necrosis are the main causes of myocardial cell loss, and cell loss through either pathway has serious consequences, such as ascites, growth retardation, decreased productive performance, and even death. To date, there has been little research on apoptosis in chicken cardiomyocytes that may eventually guide inter-

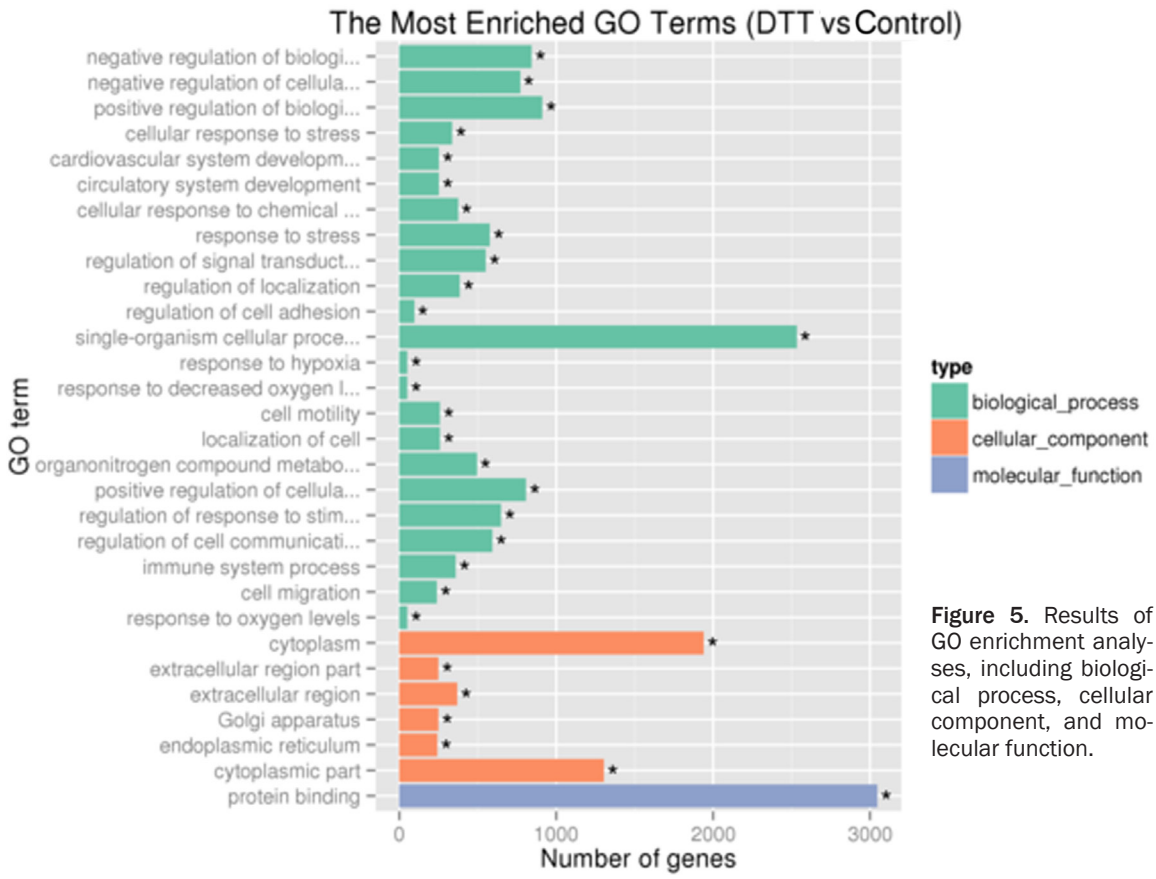

Figure 5. Results of GO enrichment analyses, including biological process, cellular component, and molecular function.

ventions to prevent prenatal cardiomyocytes during apoptosis and constructed preliminary functional signaling pathways.

At low doses, DTT can protect against oxidative stress and improve cell viability [26], while longer and higher doses induce apoptosis, possibly by *caspase-3* activation [17]. To our knowledge, ours is the first RNA-Seq study of apoptotic chicken cardiomyocytes induced using DTT. We reveal a population of differentially expressed genes that can be used to elucidate key gene pathways and other molecular processes involved in apoptosis.

Applicability of RNA-Seq for screening apoptotic response

RNA-Seq technology is a novel tool for high-throughput whole-genome or transcriptome profiling with low cost and high sensitivity and specificity [21]. In this study, we use pooled samples and replicates to further reduce spurious results. Furthermore, the quality of sequencing was monitored by error rate distribution and base content distribution. We detected 21,788 transcripts, a number similar to previous RNA-Seq studies of other eukaryote cells [21, 27]. Many of these genes were significantly differentially expressed between control and apoptotic cells. This differential gene expression dataset may contain genes responsible for induction and execution of apoptotic programs as well as cytoprotective processes. We also found novel transcripts, most without open reading frames, suggesting that the expression of many microRNAs or long non-coding RNAs is involved in control of apoptosis in avian cardiomyocytes.

Screening for apoptotic signaling pathways

We monitored certain key genes involved in each signaling pathway based on their degree of differential expression. For example, we compared the expression of *PERK*, *IRE-1* and *AIF-6* to determine whether an endoplasmic reticulum stress response is induced by DTT [22]. Indeed, differential expression between control and DTT groups indicated that DTT caused endoplasmic reticulum stress.

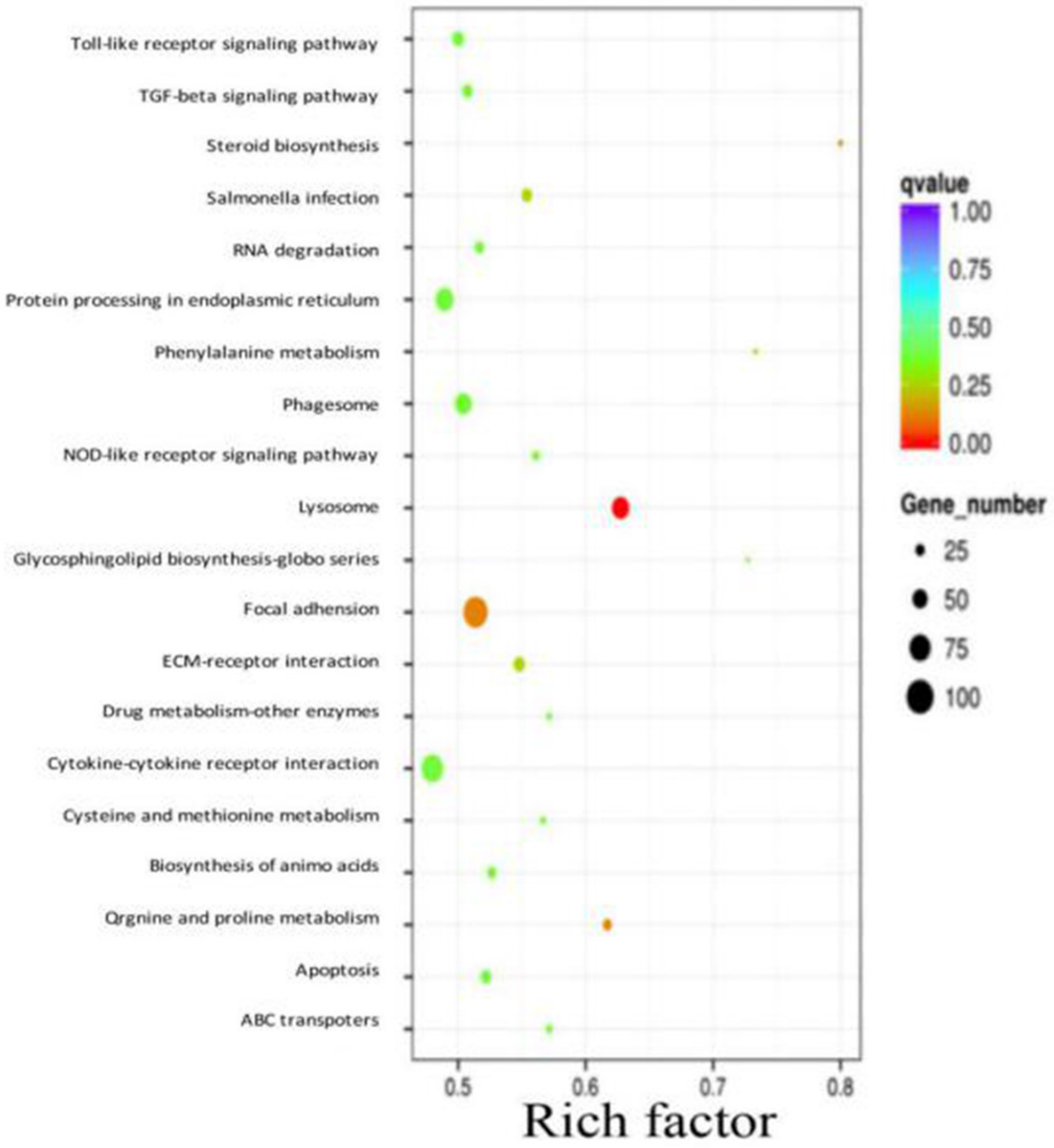

Figure 6. Statistics of KEGG enrichment. The size of each point indicates the number of differentially expressed genes in that pathway, and the color of each point indicates the *q*-value (adjusted *p* value). A higher enrichment factor indicates a greater degree of enrichment.

In HL-60 cells, DTT-induced apoptosis was independent of the mitochondria [17]. Therefore, we selected *AIF*, *CytC* and *Bax* to evaluate whether the mitochondrial pathway is involved in DTT-induced apoptosis in our system. In contrast to previous findings, our DEG analysis showed that expression levels of all three index genes were increased in the DTT group compared to the control group, suggesting that the mitochondrial pathway may be involved in DTT-induced apoptosis.

The *WNT* signaling pathway was identified through KEGG enrichment analysis. In total, 117 genes in this pathway were detected, 38 of which were significantly upregulated, including *LRP*, *GSK3*, *APC*, *Axin* and β-catenin. Thus, we conclude that the *WNT* pathway is another important pathway related to apoptosis in chicken cardiomyocytes, in accord with mammalian studies [28]. Similarly, many genes linked to the *MAPK* signaling pathway were upregulated.

KEGG analysis also identified 61 genes involved in *P53* signaling pathway, but only 28 were differentially expressed, and some key molecules showed no change in expression, such as P53-binding protein 1.

We also found that expression of several pathways with no direct relevance to apoptosis were altered, such as 'lysosome', 'steroid biosynthesis', 'phagosome', and 'NOD-like receptor signaling pathway'. We concluded these pathways may also take an important role in this apoptosis. In addition to expected differential expression of genes associated with 'response to oxygen level' and 'response to stress', and genes directly related to apoptosis, such as those grouped in 'induction of apoptosis', 'cellular component disassembly involved in execution phase of apoptosis', and/or 'negative regulation of execution phase of apoptosis', we also found that differentially expressed genes were enriched in 'protein binding' and 'regulation of cellular' groups. Therefore, the response to DTT appears to involve a complex array of signaling pathways that may involve 6468 or more genes. Nonetheless, among these are the traditional apoptosis pathways described in mammals (although this is the first report to link them to apoptosis in chickens).

Key molecules involved in the initiation, execution, and repression of apoptosis

To further investigate the initiation of apoptosis, we evaluated the expression of *caspase-2*, *caspase-8*, *caspase-9 and caspase-10* [29-31], and stage-specific effects were assessed by examining *caspase-3, caspase-6, and caspase-7* [32, 33]. Apoptosis initiation was mainly dependent on caspase-8 and caspase-9, whereas caspase-10 was downregulated, similar to the findings of Tartier [17]. Execution was mainly dependent on caspase-3. Regarding the repression of apoptosis, we compared the expression levels of the following genes: *Bcl-2*, *CFLAR*, *CAAP1*, *IAP*, *BFAR*, *TRIA1*, *API5*, and *SIVA* [34-37]. Based on differential expression, apoptosis repression in chicken cardiomyocytes may depend strongly on *Bcl-2*, *IAP* and *SIVA*. A few genes associated with suppression of apoptosis, such as *BFAR*, exhibited highly significant downregulation. The GO enrichment results also indicated that two novel genes may be involved in apoptosis repression, although this requires verification. No myocardial specificity of the anti-apoptotic gene *ARC* was observed in chickens.

Conclusion

We used RNAseq technology to screen for apoptosis-associated genes in chicken cardiomyocytes. Many novel genes and alternatively spliced transcripts were discovered among the 6,468 genes significant differentially expressed after DTT-induction. Included were genes involved in initiation, execution, and repression of apoptosis, as well as many involved in signaling pathways associated with stress responses. Initiation of this type of apoptosis was primarily dependent on *caspase-8* and *caspase-9*, whereas the execution stage was dependent on *caspase-3*. Identified signaling pathways altered by apoptosis included *WNT* and *MAPK*, while repression of apoptosis appeared primarily dependent on *Bcl-2*, *IAP* and *SIVA*. These results present possible targets for invention to improve chicken health and increase agricultural productivity.

Acknowledgements

This work was supported by a preliminary research project grant from Huazhong Agricultural University (52209-814112) and the National Natural Sciences Foundation of China (No. 31502132). The funders had no role in study design, data collection and analysis, decision to publish, or preparation of the manuscript. The authors thank Xiaona Zhang and Xiang Cui at NOVOgene (Beijing, China) for assistance with the Illumina sequencing.

Disclosure of conflict of interest

None.

Address correspondence to: Dingzong Guo, College of Veterinary Medicine, Huazhong Agricultural University, Wuhan 430070, Hubei, China. Tel: +86-27-8728-6009; E-mail: hlgdz@163.com

References

[1] Akyürek O, Akyürek N, Sayin T, Dinçer I, Berkalp B, Akyol G, Ozenci M, Oral D. Association between the severity of heart failure and the susceptibility of myocytes to apoptosis in patients with idiopathic dilated cardiomyopathy. Int J Cardiol 2001; 80: 29-36.

[2] Kang PM, Izumo S. Apoptosis in heart: basic mechanisms and implications in cardiovascu-

lar diseases. Trends Mol Med 2003; 9: 177-182.
[3] Yu J, Yang S, Wang X, Gan R. Matrine improved the function of heart failure in rats via inhibiting apoptosis and blocking β3-adrenoreceptor/endothelial nitric oxide synthase pathway. Mol Med Rep 2014; 10: 3199-3204.
[4] Tan X, Pan JQ, Li JC, Liu YJ, Sun WD, Wang XL. L-Arginine inhibiting pulmonary vascular remodelling is associated with promotion of apoptosis in pulmonary arterioles smooth muscle cells in broilers. Res Vet Sci 2005; 79: 203-209.
[5] Ashkenazi A, Dixit VM. Death receptors: signaling and modulation. Science 1998; 281: 1305-1308.
[6] Kong JY, Rabkin SW. Palmitate-induced apoptosis in cardiomyocytes ismediated through alterations in mitochonria: prevention by cyclosporine A. Biochim Biophys Acta 2000; 1485: 45-55.
[7] Danial NN, Gramm CF, Scorrano L. BAD and glucokinase reside in a mitochondrial complex that integrates glycolysis and apoptosis. Nature 2003; 424: 952-956.
[8] Fan TJ, Han LH, Cong RS, Liang J. Caspase Family Proteases and Apoptosis. Acta Biochim Biophys Sin (Shanghai) 2005; 37: 719-727.
[9] Geertman R, McMahon A, Sabban EL. Cloning and characterization of cDNAs for novel proteins with glutamic acid-proline dipeptide tandem repeats. Biochim Biophys Acta 1996; 1306: 147-152.
[10] Hampton M, Melvin RG, Andrews MT. Transcriptomic analysis of brown adipose tissue across the physiological extremes of natural hibernation. PLoS One 2013; 8: e85157.
[11] Tamim S, Vo DT, Uren PJ, Qiao M, Bindewald E, Kasprzak WK, Shapiro BA, Nakaya HI, Burns SC, Araujo PR, Nakano I, Radek AJ, Kuersten S, Smith AD, Penalva LO. Genomic analyses reveal broad impact of miR-137 on genes associated with malignant transformation and neuronal differentiation in glioblastoma cells. PLoS One 2014; 9: e85591.
[12] Schunter C, Vollmer SV, Macpherson E, Pascual M. Transcriptome analyses and differential gene expression in a non-model fish species with alternative mating tactics. BMC Genomics 2014; 15: 167.
[13] Connell S, Meade KG, Allan B, Lloyd AT, Kenny E, Cormican P, Morris DW, Bradley DG, O'Farrelly C. Avian resistance to Campylobacter jejuni colonization is associated with an intestinal immunogene expression signature identified by mRNA sequencing. PLoS One 2012; 7: e40409.
[14] Fukuda K. Current status of myocardial regeneration and cell transplantation. Future Cardiol 2005; 1: 167-175.
[15] Solaini G, Harris DA. Biochemical dysfunction in heart mitochondria exposed to ischaemia and reperfusion. Biochem J 2005; 390: 377-394.
[16] Takeuchi T. Regulation of cardiomyocyte proliferation during development and regeneration. Dev Growth Differ 2014; 56: 402-409.
[17] Tartier L, McCarey YL, Biaglow JE, Kochevar IE, Held KD. Apoptosis induced by dithiothreitol in HL-60 cells shows early activation of caspase 3 and is independent of mitochondria. Cell Death Differ 2000; 7: 1002-1010.
[18] DeHaan RL. Development of form in the embryonic heart, An experimental approach. Circulation 1967; 35: 821-833.
[19] Volz A, Piper HM, Siegmund B, Schwartz P. Longevity of adult ventricular rat heart muscle cells in serum-free primary culture. J Mol Cell Cardiol 1991; 23: 161-173.
[20] Taber LA, Hu N, Pexieder T, Clark EB, Keller BB. Residual strain in the ventricle of the stage 16-24 chick embryo. Circ Res 1993; 72: 455-462.
[21] Mortazavi A, Williams BA, McCue K, Schaeffer L, Wold B. Mapping and quantifying mammalian transcriptomes by RNA-Seq. Nat Methods 2008; 5: 621-628.
[22] Akazawa Y, Isomoto H, Matsushima K, Kanda T, Minami H, Yamaghchi N, Taura N, Shiozawa K, Ohnita K, Takeshima F, Nakano M, Moss J, Hirayama T, Nakao K. Endoplasmic reticulum stress contributes to Helicobacter pylori VacA-induced apoptosis. PLoS One 2013; 8: e82322.
[23] Renfro DP, McIntosh BK, Venkatraman A, Siegele DA, Hu JC. GONUTS: the Gene Ontology Normal Usage Tracking System. Nucleic Acids Res 2012; 40: D1262-D1269.
[24] Mao X, Cai T, Olyarchuk JG, Wei L. Automated genome annotation and pathway identification using the KEGG Orthology (KO) as a controlled vocabulary. Bioinformatics 2005; 21: 3787-3793.
[25] Kanehisa M, Araki M, Goto S, Hattori M, Hirakawa M, Itoh M, Katayama T, Kawashima S, Okuda S, Tokimatsu T, Yamanishi YI. KEGG for linking genomes to life and the environment. Nucleic Acids Res 2008; 36: D480-D484.
[26] Rao B, David G. Improved recovery of post-thaw motility and vitality of human spermatozoa cryopreserved in the presence of dithiothreitol. Cryobiology 1984; 21: 536-541.
[27] Marioni JC, Mason CE, Mane SM, Stephens M, Gilad Y. RNAseq: an assessment of technical reproducibility and comparison with gene expression arrays. Genome Res 2008; 18: 1509-1517.
[28] Bodine PV. Wnt signalingcontrol of bone cell apoptosis. Cell Res 2008; 18: 248-253.
[29] Grossmann J, Walther K, Artinger M, Kiessling S, Schölmerich J. Apoptotic signaling during

initiation of detachment-induced apoptosis ("anoikis") of primary human intestinal epithelial cells. Cell Growth Differ 2001; 12: 147-155.

[30] Mueller T, Voigt W, Simon H, Fruehauf A, Bulankin A, Grothey A, Schmoll HJ. Failure of activation of caspase-9 induces a higher threshold for apoptosis and cisplatin resistance in testicular cancer. Cancer Res 2003; 63: 513-521.

[31] Chang GC, Hsu SL, Tsai JR, Liang FP, Lin SY, Sheu GT, Chen CY. Molecular mechanisms of ZD1839-induced G1-cell cycle arrest and apoptosis in human lung adenocarcinoma A549 cells. Biochem Pharmacol 2004; 68: 1453-1464.

[32] Gregoli PA, Bondurant MC. Function of caspases in regulating apoptosis caused by erythropoietin deprivation in erythroid progenitors. J Cell Physiol 1999; 178: 133-143.

[33] Lee CJ, Liao CL, Lin YL. Flavivirus activates phosphatidylinositol 3-kinase signaling to block caspase-dependent apoptotic cell death at the early stage of virus infection. J Virol 2005; 79: 8388-8399.

[34] Chao DT, Linette GP, Boise LH, White LS, Thompson CB, Korsmeyer SJ. Bcl-XL and Bcl-2 repress a common pathway of cell death. J Exp Med 1995; 182: 821-828.

[35] Fortin A, MacLaurin JG, Arbour N, Cregan SP, Kushwaha N, Callaghan SM, Park DS, Albert PR, Slack RS. The proapoptotic gene SIVA is a direct transcriptional target for the tumor suppressors p53 and E2F1. J Biol Chem 2004; 279: 28706-28714.

[36] Zhang Y, Johansson E, Miller ML, Jänicke RU, Ferguson DJ, Plas D, Meller J, Anderson MW. Identification of a conserved anti-apoptotic protein that modulates the mitochondrial apoptosis pathway. PLoS One 2011; 6: e25284.

[37] Furukawa J, Miyake H, Fujisawa M. Upregulation of anti-apoptotic gene. Nihon Rinsho 2011; 69 Suppl 5: 117-120.